J. Fluid Mech. (2021), *vol*. 908, A22. © The Author(s), 2020.
Published by Cambridge University Press
doi:10.1017/jfm.2020.873

The unsteady lift of an oscillating airfoil encountering a sinusoidal streamwise gust

Ruwei Ma[1], **Yang Yang**[1,2], **Mingshui Li**[1,2,†] **and Qiusheng Li**[3,†]

[1]Research Centre for Wind Engineering, Southwest Jiaotong University, Chengdu 610031, PR China

[2]Key Laboratory for Wind Engineering of Sichuan Province, Chengdu 610031, PR China

[3]Department of Architecture and Civil Engineering, City University of Hong Kong, Kowloon, Hong Kong

(Received 3 July 2020; revised 4 September 2020; accepted 8 October 2020)

The unsteady lift of an oscillating airfoil encountering a sinusoidal streamwise gust is experimentally investigated. The sinusoidal streamwise gust is generated by a multiple-fan actively controlled wind tunnel. A two-dimensional airfoil with a NACA0015 profile oscillates in the wind tunnel with a pitch motion frequency of $f_v = 1$ Hz while the sinusoidal streamwise gust has a different oscillating frequency of $f_\beta = 1.7$ Hz. The non-dimensional unsteady lift coefficients determined from surface pressure show the same trends as Greenberg's prediction. Through spectral analysis, the sum frequency $f_{sum} = f_\beta + f_v$ and the difference frequency $f_{diff} = |f_\beta - f_v|$, proposed by Greenberg, are firstly observed in the experiment. The experimental results are compared with Greenberg's theory in the case of a small amplitude of gust velocity variation $\sigma = 0.2$. The results of all cases indicate that the experimental results agree generally well with Greenberg's prediction, while there is a small deviation.

Key words: flow–structure interactions

1. Introduction

An airfoil encountering a highly unsteady flow is a classical fluid dynamics issue because of the time-varying part of flow velocity. This issue involves some significant problems like flutter, unsteady lift of an airfoil and loading on turbomachines (Barlas & Van Kuik 2010; van Kuik *et al.* 2014). Although the relevant problems have been discussed for many years, it is still difficult to calculate the aerodynamic loads accurately. Such information is necessary for predicting the aeroelastic behaviour of an airfoil.

As early as 1935, Theodorsen (1935) proposed the fundamental solution for an airfoil oscillating in a steady free stream. The validity of his theory has been verified by many experimental investigations (Silverstein & Joyner 1939; Reid 1940; Halfman 1952; Rainey 1957), but the application of Theodorsen's theory to a helicopter blade is questionable (Johnson 1980), because of the bidimensionality of the flow and the largely nonlinear structural or aerodynamic phenomena. Sears (1941) analysed the transient lift development of an airfoil in a transverse gust by following the earlier work of non-uniform motion (von Karman & Sears 1938), and then calculated the fluctuations in lift of the rotors

† Email addresses for correspondence: lms_rcwe@126.com, bcqsli@cityu.edu.hk

and stators of axial flow turbomachines (Kemp & Sears 1953, 1955). Isaacs (1945) was probably the first to calculate the lift force on an airfoil for the need of more accurate estimations of helicopter blade loads. He provided a complete solution to the lift force of an airfoil with constant attack angle when the incoming flow has variable magnitude. But for the case of variable attack angle, which is undeniably of importance for rotary wing aircraft, relevant calculations were not undertaken. About the same time, Greenberg (1947) developed a simplified solution for this case using a different method. He assumed a simple form of wake with a certain degree of approximation by extending the method of Theodorsen (1935) and obtained the lift on an airfoil not only in a sinusoidal streamwise gust but also in pitching and plunging motions. Kottapalli (1985) developed a similar theory for the same problem by assuming small pitching oscillation amplitudes with respect to the mean flow velocity. van der Wall & Leishman (1994) compared the theories of Isaacs (1945), Greenberg (1947) and Kottapalli (1985), and concluded that the theory of Isaacs is the only exact theory without additional simplification and extended the theory to arbitrary free-stream velocity variations and arbitrary motions. It must be noted that all these theoretical approaches are based on certain assumptions: incompressible potential flow, two-dimensional flat-plate airfoil, attached flow, planar and non-deforming wake and small disturbances.

As summarized above, the relevant theories for this classical issue have been developed for decades, but most of them have not been fully validated by experiments (Leishman 2002), especially the theory of Greenberg (1947), which has been widely used in applications for many years. Favier *et al.* (1988) investigated the unsteady lift of a pitching airfoil in an unsteady free stream with moderate velocity amplitudes, but the experimental results were not compared with any theoretical prediction. Granlund *et al.* (2014) experimentally investigated the unsteady lift of a fixed NACA0009 airfoil in time-periodic sinusoidal gusts with a constant attack angle. Their experimental results agreed well with Greenberg's theory at small attack angles while there was a marked deviation at large attack angles. Strangfeld *et al.* (2016) investigated a two-dimensional airfoil encountering a harmonic oscillation flow with high amplitude at constant attack angle using both theoretical calculations and experiments. They concluded that the method of Isaacs is more accurate compared with Greenberg's theory. However, most experimental investigations mentioned above focused on a fixed airfoil with a constant attack angle. But for an oscillating airfoil subject to a harmonic oscillation incoming flow, which was also derived by Greenberg (1947), relevant studies are still scarce. One important reason of this lack is probably due to the fact that such a pure harmonic oscillation flow is difficult to produce in a conventional wind tunnel. The most common approach for solving this problem is to modify a conventional wind tunnel (Szumowski & Meier 1996; Harding, Payne & Bryden 2014). Another approach is using a louvre system (Kerstens *et al.* 2011; Granlund *et al.* 2014; Monnier *et al.* 2016; Strangfeld *et al.* 2016). The quality of sinusoidal gusts for the first approach is limited by the effects of fan stall and large inertia. For the second approach, the louvre system would produce a pressure gradient that might cause an extra component of pressure on the airfoil. In that case, a multiple-fan actively controlled wind tunnel, which is specially designed for the purpose of producing a streamwise fluctuating flow, is an idea facility.

In this study, the unsteady lift on an oscillating airfoil encountering a sinusoidal streamwise gust is investigated using a multiple-fan actively controlled wind tunnel. The quality of the generated fluctuating flow was proved to be excellent (Yang *et al.* 2017). The surface pressures of the airfoil are measured using DMS-4000 pressure scanners, and

thus the lift force can be obtained by integration along the chord length of the airfoil. Experimental results of this study are compared with Greenberg's prediction. Using spectral analysis, the reasons for the small deviation between the experimental results and the theoretical results are discussed.

2. Theoretical description

Fundamental solutions for an oscillating airfoil in a steady free stream were given by Theodorsen (1935). The validity of his theory has been verified by several experiments (Silverstein & Joyner 1939; Reid 1940; Halfman 1952; Rainey 1957). For an airfoil in harmonic pitch oscillation, the unsteady lift is

$$F = \pi\rho b^2\left(v\dot{\beta} - b\bar{a}\ddot{\beta}\right) + 2\pi\rho v b C(k)\left[v\beta + b\left(\tfrac{1}{2} - \bar{a}\right)\dot{\beta}\right], \tag{2.1}$$

where ρ is the air density, b is the half-chord of the airfoil, v is the streamwise wind velocity, $\bar{a}$ is the non-dimensional position of torsion axis of the airfoil measured from the centre, $\beta = \beta_0\cos(2\pi f_\beta t)$ is pure pitch motion and $C(k)$ is the well-known Theodorsen function.

Theodorsen's theory was based on the following assumptions: incompressible potential flow, two-dimensional flat-plate airfoil, planar and non-deforming wake, small disturbances and attached flow. To extend that theory to an unsteady fluctuation stream, simply replacing the constant wind velocity v by fluctuation velocity $v = v_0(1 + \sigma\sin(2\pi f_v t))$ is not enough. The effect on both non-circulatory and circulatory forces should also be considered. On that basis, Greenberg (1947) extended Theodorsen's theory to the case of an oscillating airfoil encountering a periodically varying streamwise flow.

For the non-circulatory part, adding the effect of time-varying velocity and integrating the pressure difference over the entire airfoil gives the total non-circulatory force:

$$L_{nc} = \pi\rho b^2\left[v\dot{\beta} + \dot{v}(\alpha + \beta) - b\bar{a}\ddot{\beta}\right]. \tag{2.2}$$

While the non-circulatory moment is

$$M_{nc} = \pi\rho b^2\left[-v^2(\alpha + \beta) - b\bar{a}\dot{v}(\alpha + \beta) + b^2\left(\tfrac{1}{8} + \bar{a}^2\right)\ddot{\beta}\right]. \tag{2.3}$$

For the circulatory part, Greenberg made an assumption of high frequency to the wake velocity, which gives the wake a pure periodic form to simplify the derivation. Although the assumption of high frequency for the wake integrals is questionable, it is concluded to be equivalent to a small σ approximation for parts of the wake (van der Wall & Leishman 1994). On that basis, the circulatory force can be derived as

$$\begin{aligned} L_c = 2\pi\rho v b\Big\{&v_0\alpha + \sigma v_0\alpha C(k_v)\mathrm{e}^{\mathrm{i}\omega_v t} + \left[\mathrm{i}\omega_\beta\beta_0 b\left(\tfrac{1}{2} - \bar{a}\right) + v_0\beta_0\right]C(k_\beta)\mathrm{e}^{\mathrm{i}\omega_\beta t} \\ &+ \sigma v_0\beta_0 C(k_{v+\beta})\mathrm{e}^{\mathrm{i}(\omega_v+\omega_\beta)t}\Big\}, \end{aligned} \tag{2.4}$$

where $k_v = 2\pi f_v b/v_0$, $k_\beta = 2\pi f_\beta b/v_0$ and $k_{v+\beta} = 2\pi f_{v+\beta} b/v_0$. Using the same method, the circulatory moment is

$$\begin{aligned} M_c = \pi\rho v b^2\left[v(\alpha + \beta) + \dot{\beta}b\left(\tfrac{1}{2} - \bar{a}\right)\right] - 2\pi\rho v b^2\left(\tfrac{1}{2} + \bar{a}\right)\Big\{&v_0\alpha + \sigma v_0\alpha C(k_v)\mathrm{e}^{\mathrm{i}\omega_v t} \\ &+ \left[b\left(\tfrac{1}{2} - \bar{a}\right)\dot{\beta} + v_0\beta\right]C(k_\beta) + \sigma v_0\beta C(k_{v+\beta})\mathrm{e}^{\mathrm{i}\omega_v t}\Big\}. \end{aligned} \tag{2.5}$$

Adding (2.2) and (2.4) gives the total lift force:

$$L = \pi\rho b^2\left[v\dot{\beta} + \dot{v}(\alpha+\beta) - b\bar{a}\ddot{\beta}\right] + 2\pi\rho v b\left\{v_0\alpha + \sigma v_0\alpha C(k_v)\mathrm{e}^{\mathrm{i}\omega_v t}\right.$$
$$\left. + \left[b\left(\tfrac{1}{2}-\bar{a}\right)\dot{\beta} + v_0\beta\right]C(k_\beta) + \sigma v_0\beta C(k_{v+\beta})\mathrm{e}^{\mathrm{i}\omega_v t}\right\}. \tag{2.6}$$

Adding (2.3) and (2.5) gives the total moment:

$$M = \pi\rho b^2\left[vb\left(\tfrac{1}{2}-\bar{a}\right)\dot{\beta} - b\bar{a}\dot{v}(\alpha+\beta) + b^2\left(\tfrac{1}{8}+\bar{a}^2\right)\ddot{\beta}\right]$$
$$- 2\pi\rho v b^2\left(\tfrac{1}{2}+\bar{a}\right)\left\{v_0\alpha + \sigma v_0\alpha C(k_v)\mathrm{e}^{\mathrm{i}\omega_v t}\right.$$
$$\left. + \left[b\left(\tfrac{1}{2}-\bar{a}\right)\dot{\beta} + v_0\beta\right]C(k_\beta) + \sigma v_0\beta C(k_{v+\beta})\mathrm{e}^{\mathrm{i}\omega_v t}\right\}. \tag{2.7}$$

For the case of pure harmonic pitch oscillation without constant attack angles:

$$L_s = \pi\rho b^2\left[v\dot{\beta} + \dot{v}\beta - b\bar{a}\ddot{\beta}\right]$$
$$+ 2\pi\rho v b\left\{\left[b\left(\tfrac{1}{2}-\bar{a}\right)\dot{\beta} + v_0\beta\right]C(k_\beta) + \sigma v_0\beta C(k_{v+\beta})\mathrm{e}^{\mathrm{i}\omega_v t}\right\}, \tag{2.8}$$

$$M = \pi\rho b^2\left[vb\left(\tfrac{1}{2}-\bar{a}\right)\dot{\beta} - b\bar{a}\dot{v}\beta + b^2\left(\tfrac{1}{8}+\bar{a}^2\right)\ddot{\beta}\right]$$
$$- 2\pi\rho v b^2\left(\tfrac{1}{2}+\bar{a}\right)\left\{\left[b\left(\tfrac{1}{2}-\bar{a}\right)\dot{\beta} + v_0\beta\right]C(k_\beta) + \sigma v_0\beta C(k_{v+\beta})\mathrm{e}^{\mathrm{i}\omega_v t}\right\}. \tag{2.9}$$

After normalizing all dynamic effects, the non-dimensional lift coefficient is

$$C_L = \frac{L_s}{2\pi\rho b {v_0}^2\beta_0}, \tag{2.10}$$

$$C_M = \frac{L_s}{4\pi\rho b^2 {v_0}^2\beta_0}. \tag{2.11}$$

It should be noticed that there are three frequencies included in the unsteady lift development, which are the frequency of harmonic pitch oscillation f_β, the sum frequency $f_{sum} = f_\beta + f_v$ and the difference frequency $f_{diff} = |f_\beta - f_v|$ generated by the product of $\sin(2\pi f_v t))$ and $\cos(2\pi f_\beta t)$. However, as far as we know, no experimental research has reported the existence of the sum frequency and difference frequency. A relevant study set the gust fluctuation frequency the same as the model oscillating frequency in experiments for consideration of engineering applications (Strangfeld *et al.* 2015).

3. Experimental set-up

3.1. *Sinusoidal streamwise gust*

The experiment was conducted in the multiple-fan actively controlled wind tunnel of the State Key Laboratory of Disaster Reduction in Civil Engineering at Tongji University, Shanghai, China. Unlike conventional wind tunnels, this actively controlled wind tunnel has 120 individual fans arranged in a 10×12 matrix to produce specific forms of flow, including a sinusoidal streamwise gust. Each fan can work independently and is controlled by computer. By inputing specific parameters, a sinusoidal streamwise gust $v = v_0(1 + \sigma\sin(2\pi f_v t))$ can be generated with predetermined oscillation frequency f_v, mean flow velocity v_0 and amplitude of velocity variation σ. Figure 1 shows a comparison of the measured streamwise gust with the targeted streamwise velocity. The oscillation frequency is $f_v = 1$ Hz. It is clear from figure 1(*a*) that the two velocity time histories match

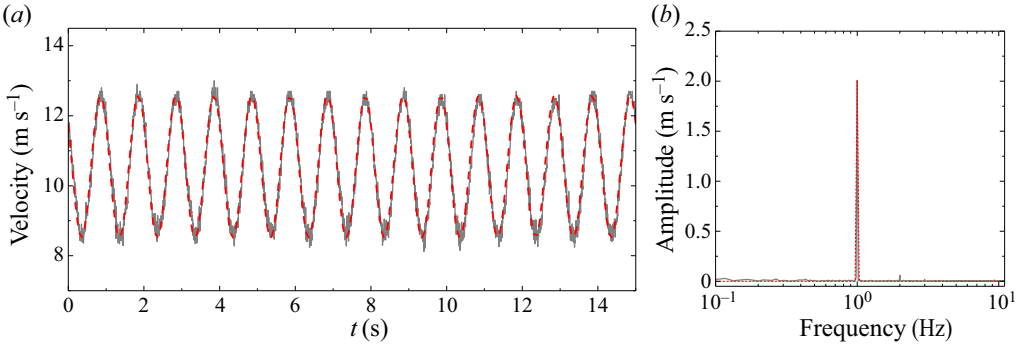

FIGURE 1. (*a*) Time history of the sinusoidal streamwise gust. (*b*) The corresponding Fourier amplitude spectrum of the gust. The grey line is the measured signal while the red dashed line is the expected velocity. Here $v_{0,measured} = 10.6\ \mathrm{m\,s^{-1}}$, $v_{0,ideal} = 10.5\ \mathrm{m\,s^{-1}}$, $\sigma_{ideal} = 0.2$, $\sigma_{measured} = 0.196, f_v = 1$ Hz.

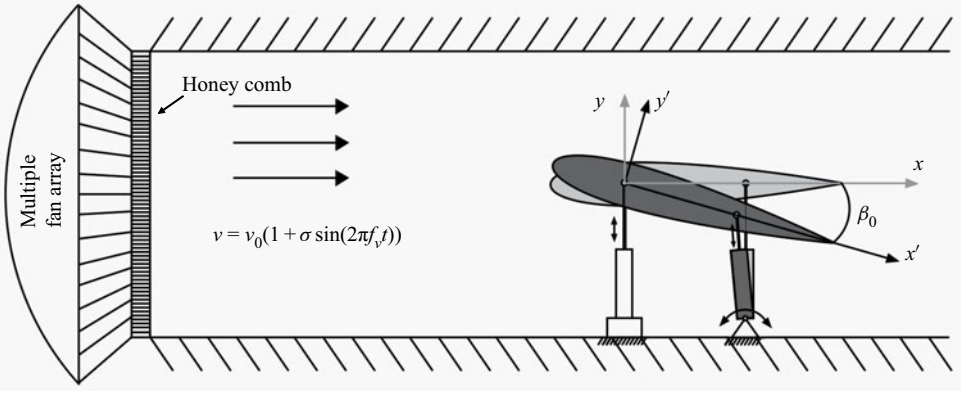

FIGURE 2. Sketch of experimental set-up for an oscillating airfoil encountering a sinusoidal streamwise gust.

very well. The ideal mean stream velocity is $v_{0,ideal} = 10.5\ \mathrm{m\,s^{-1}}$ while the measured mean stream velocity is $v_{0,measured} = 10.6\ \mathrm{m\,s^{-1}}$. The expected amplitude of velocity variation is $\sigma_{ideal} = 0.2$ while the measured one is $\sigma_{measured} = 0.196$, resulting in a difference of 2 %. Figure 1(*b*) shows the spectral analysis of the two time histories of velocity. It is obvious that there is only one marked peak in the spectra, which is consistent with the expected oscillation frequency $f_v = 1$ Hz. Therefore, the sinusoidal streamwise gust produced by the multiple-fan actively controlled wind tunnel is of good quality.

3.2. *Oscillating airfoil*

Figure 2 shows a schematic of the experimental set-up. A two-dimensional NACA0015 airfoil is oscillating in the multiple-fan actively controlled wind tunnel. The NACA0015 airfoil has a chord length of $2b = 0.4$ m and a span of $s = 1.2$ m while the test section of the wind tunnel is 1.5 m × 1.8 m. A forced-oscillation rig is installed in the test section to make the airfoil oscillate in the sinusoidal streamwise gust. The forced-oscillation rig consists of four linear actuators and each actuator can work independently. With a phase difference of π between the front actuators and rear actuators, the airfoil can

oscillate in pure pitch motion $\beta = \beta_0 \cos(2\pi f_\beta t)$ of amplitude β_0 and frequency f_β. To measure the surface pressure distribution of the airfoil, two chord-wise strips are set on the airfoil surface, each strip having 48 taps. These two strips are connected to DMS-4000 pressure scanners, which can acquire the dynamic pressure. Integration along the chord length of the airfoil gives the total lift force $F = \sum P_i L_i \cos\theta_i$. Here P_i is the pressure of point i, L_i is the integral length of point i and θ_i is the angle between the inner normal and the horizontal plane.

In order to identify the sum frequency $f_{sum} = f_\beta + f_v$ and the difference frequency $f_{diff} = |f_\beta - f_v|$, the pitch motion frequency is set as $f_\beta = 1.4$ and 1.7 Hz to differ from the frequency of the sinusoidal streamwise gust $f_v = 1$ Hz. The pitch angles are $\beta_0 = 1^\circ$ and 2°.

4. Results and discussion

Figure 3 shows a comparison between the measured phase-averaged unsteady lift coefficient and the theoretical prediction of Greenberg (1947). Because of the difference in frequency between stream oscillation and pitch motion, there should be three frequencies included in the lift development. In that case, the unsteady lift is not harmonic and each pitch motion cycle is different. Figures 3(*a*) and 3(*b*) show the results of the first six cycles of pitch motion for $f_\beta = 1.4$ and 1.7 Hz, respectively. It should be noticed that for pitch motion frequency $f_\beta = 1.7$ Hz, the whole period of the lift development has 17 pitch motion cycles, which also contains 27 cycles of sum frequency and 7 cycles of difference frequency. Similarly, for pitch motion frequency $f_\beta = 1.4$ Hz, the whole period of the lift development has 7 pitch motion cycles, which contains 12 cycles of sum frequency and 2 cycles of difference frequency. In general, the experimental results in figure 3 are in good agreement with the theoretical prediction and all three curves have exactly the same trend. It is clear that the non-dimensional lift is nearly the same for the two different pitching amplitudes ($\beta_0 = 1^\circ$ and 2°), but the difference between the experimental results and the theoretical prediction should not be ignored. For pitching frequency $f_\beta = 1.4$ Hz, the deviation is obvious in the range $90^\circ < \phi < 270^\circ$, in cycle 1. In cycle 4, the same deviation can be seen in the same range. For pitching frequency $f_\beta = 1.7$ Hz, it can be seen clearly that the period of motion is different from that of $f_\beta = 1.4$ Hz, which means the component at pitch motion frequency has a significant effect on the lift development. However, similar deviation can also be seen in the range $90^\circ < \phi < 270^\circ$ in cycles 1 and 3. It can be concluded that the difference between the experimental results and the theoretical prediction shows a kind of periodicity.

In order to study the specific reason for the deviation between the experimental results and the theoretical prediction, spectral analysis is conducted to compare the amplitude of each part directly. Figure 4 shows the corresponding Fourier amplitude spectrum of the unsteady lift coefficient. As predicted by the Greenberg theory, the sum frequency $f_{sum} = f_\beta + f_v$ and the difference frequency $f_{diff} = |f_\beta - f_v|$ can be seen obviously in the experimental results. As far as we know, this is the first time for these two frequencies being observed in experiments. The results show that the amplitude of pitch motion frequency f_β is very close to the theoretical value, which is mainly affected by the mean velocity of the incoming flow. For the amplitudes of the sum frequency f_{sum} and the difference frequency f_{diff}, which are also affected by the fluctuation intensity of the incoming flow, results are quite different. The amplitude of the sum frequency f_{sum} is also very close to the theoretical value while the amplitude of the difference frequency f_{diff} has a significant error. In addition, there is another obvious peak in the experimental results,

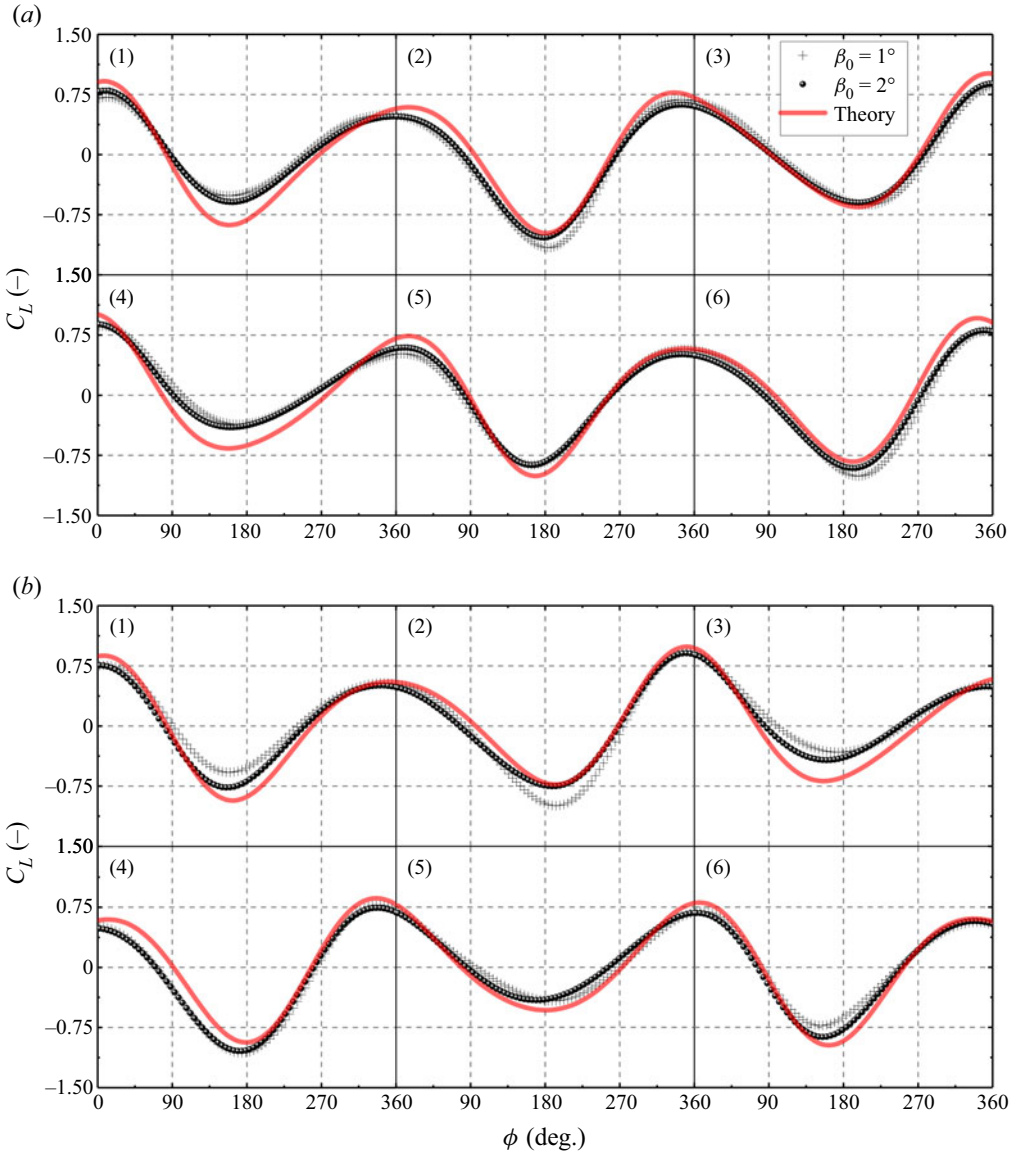

FIGURE 3. Time history of non-dimensional unsteady lift coefficient of the first six cycles. The airfoil is pitched continuously with amplitude $\beta_0 = 1°$ and $2°$. The sinusoidal incoming flow is $v = v_0(1 + \sigma \sin(2\pi f_v t))$ with $v_0 = 10.6\ \mathrm{m\,s^{-1}}$, $\sigma = 0.2$ and $f_v = 1$ Hz. (*a*) Pitch motion frequency is $f_\beta = 1.4$ Hz. (*b*) Pitch motion frequency is $f_\beta = 1.7$ Hz. Experimental results are compared with Greenberg's prediction, which is represented by red solid line. Markers (1)–(6) represent cycles 1–6, respectively.

which has the same frequency as the sinusoidal streamwise gust. The reason for such a frequency component is probably due to the existence of a small steady attack angle, which is almost inevitable in such an actively controlled wind tunnel.

Figure 4 indicates that the frequency component of pitching frequency, the sum frequency and the difference frequency are dominant in the unsteady lift. To discuss

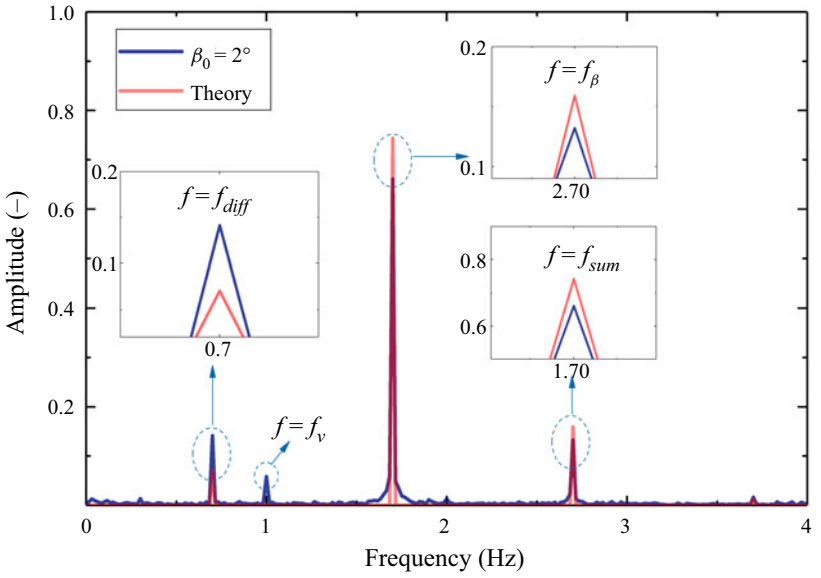

FIGURE 4. The Fourier amplitude spectrum of the unsteady lift coefficient. Pitch motion frequency $f_\beta = 1.7$ Hz, sinusoidal streamwise gust frequency $f_v = 1$ Hz, sum frequency $f_{sum} = 2.7$ Hz and difference frequency $f_{diff} = 0.7$ Hz. The parameters of the sinusoidal streamwise gust are: $v_0 = 10.6\ \mathrm{m\,s^{-1}}$, $\sigma = 0.2$ and $f_v = 1$ Hz. Experimental results for $\beta_0 = 2°$, represented by blue solid line, are compared with Greenberg's prediction, represented by red solid line.

the difference of each part between the experimental results and theoretical values, the amplitudes and phases of different pitch motion frequency ($f_\beta = 1.4$ and 1.7 Hz), sum frequency f_{sum} and difference frequency f_{diff} are given in figures 5 and 6, respectively. Each plot represents the amplitude of every 'dominant' harmonic in the unsteady lift. Here the reduced frequencies are varying by changing the mean flow speed and keeping pitch frequencies constant. In each group of plots, the correlation of the theoretical results with the experimental results is good. The amplitude of non-dimensional lift coefficient of each frequency has the same variation trend as Greenberg's theory. To be specific, the amplitudes of the experimental results agree well with the theoretical values for the pitching frequency component, as shown in figures 5(*a*) and 6(*a*). The small deviation is probably due to the effect of the thickness of the NACA0015 airfoil (Glegg & Devenport 2009; Motta, Guardone & Quaranta 2015). Experimental results of phase angles of unsteady loads with respect to motion are also shown in figures 5(*a*) and 6(*a*). It can be seen that the agreement between the theoretical and experimental results is generally good according to the plots. Moreover, the non-dimensional lift is nearly the same for the two different pitching amplitudes. This is in accordance with linear theory with respect to the pitching amplitude for the range of pitching amplitudes considered, and in good agreement with the findings of Halfman (1952). This also implies that any offset in the steady angle of attack is likely to have a small effect. Figures 5(*b*) and 6(*b*) show a comparison of amplitudes for the sum frequency component. The agreement between the experimental results and theoretical predictions for $f_\beta = 1.4$ and 1.7 Hz is still reasonably good. The variation tendencies with the reduced frequencies for the theoretical predictions and experimental results of both $\beta_0 = 1°$ and $2°$ are identical. Moreover, the correlation of the theoretical results with the experimental results for phase angles is also good.

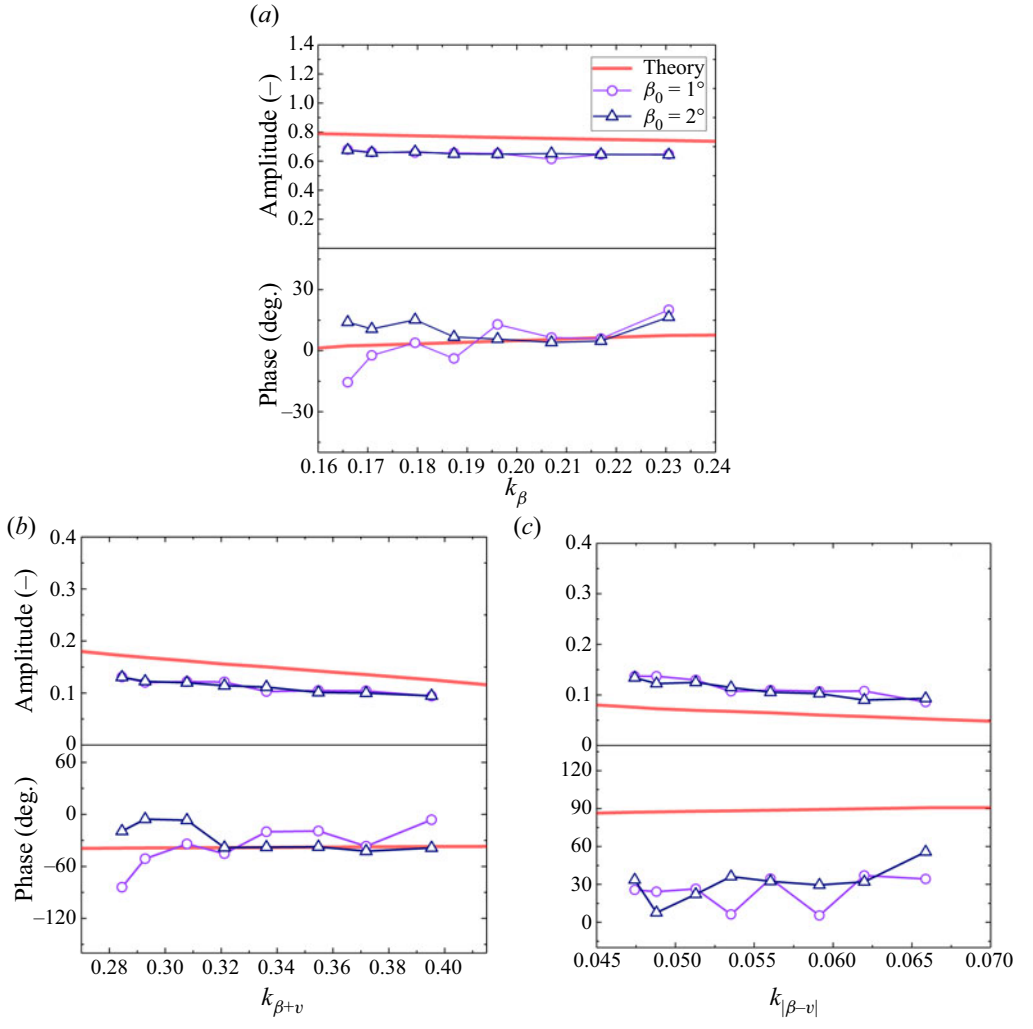

FIGURE 5. Normalized lift amplitudes of (*a*) pitch motion frequency f_β, (*b*) sum frequency f_{sum} and (*c*) difference frequency f_{diff} with different reduced frequency. Here $f_\beta = 1.4$ Hz, $k_\beta = 2\pi f_\beta b/v_0$, $k_{\beta+v} = 2\pi f_{sum} b/v_0$, $k_{|\beta-v|} = 2\pi f_{diff} b/v_0$.

Both experimental results and theoretical prediction of phase angles have the same variation tendency, with the difference being very small for the motion frequency component and the sum frequency component. However, for the difference frequency component, as shown in figures 5(*c*) and 6(*c*), the difference between the experimental results and theoretical prediction is relatively marked. It can be seen that the amplitudes of f_{diff} have similar values to those of f_{sum} while Greenberg's theory indicates that the amplitudes of f_{sum} should be larger than those of f_{diff}. In addition, deviation of phase angles between the experimental results and theoretical prediction is also significant according to the plots. However, the absolute difference between the theoretical and experimental results of the lift in figures 5(*a*) and 6(*a*) is about the same as that in figures 5(*c*) and 6(*c*). Thus, the lift coefficient still agrees well with Greenberg's theory in general. It can be concluded that the agreement between theory and experiment is best

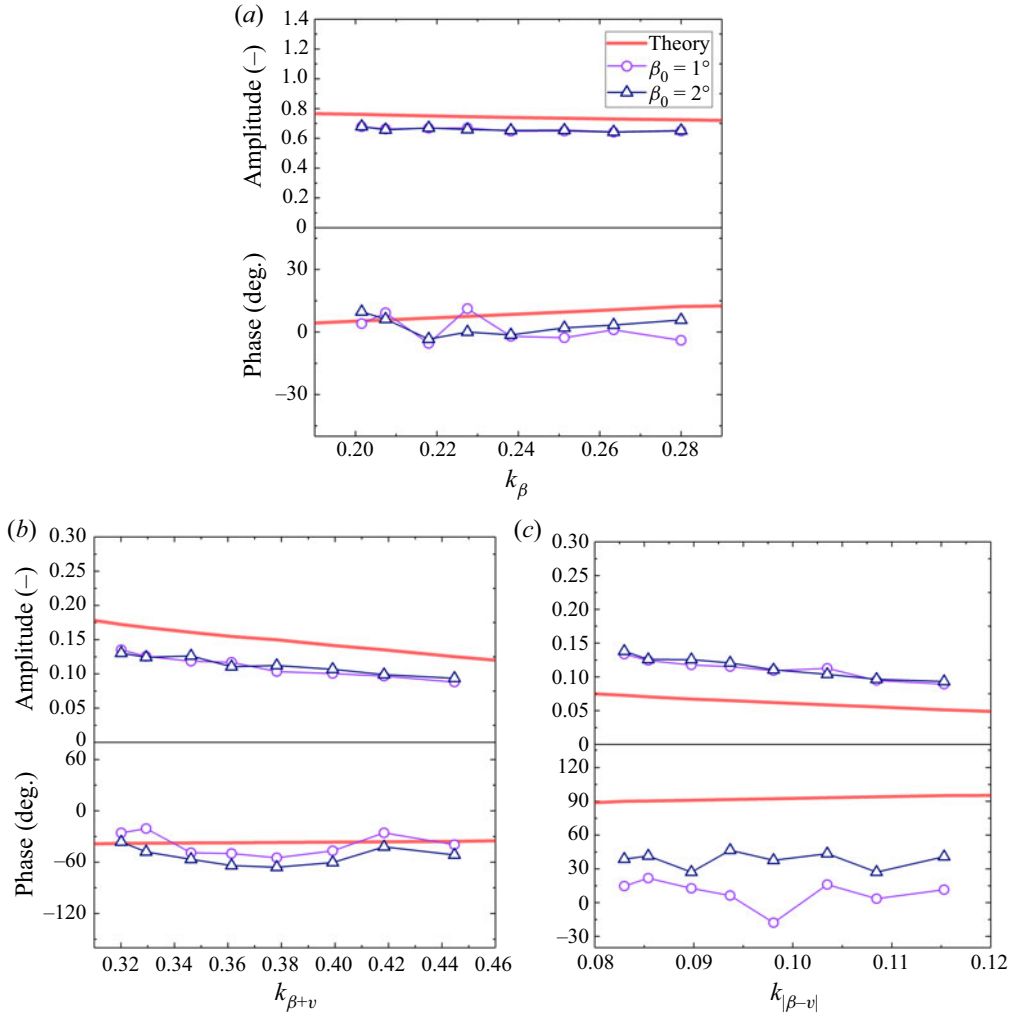

FIGURE 6. Normalized lift amplitudes of (*a*) pitch motion frequency f_β, (*b*) sum frequency f_{sum} and (*c*) difference frequency f_{diff} with different reduced frequency. Here $f_\beta = 1.7$ Hz, $k_\beta = 2\pi f_\beta b/v_0$, $k_{\beta+v} = 2\pi f_{sum} b/v_0$, $k_{|\beta-v|} = 2\pi f_{diff} b/v_0$.

for the frequency component of pitching frequency, and still reasonably good for the sum frequency component and least good for the difference frequency component, since that is also the order of the relative magnitudes of the lifts at each of these frequency components.

Figures 7 and 8 show the amplitudes and phase angles of moment coefficient of pitching frequency $f_\beta = 1.4$ and 1.7 Hz with different reduced frequencies, which are varying by changing the mean flow speed and keeping pitch frequencies constant. In general, the correlation between the theoretical results and the experimental results is good. Similar to the plots of lift coefficient in figures 5 and 6, the amplitude of non-dimensional lift coefficient of each frequency has the same variation trend as Greenberg's theory. The experimental results of the pitching frequency component agree well with the theoretical values, as shown in figures 7(*a*) and 8(*a*). Plots of phase angles of unsteady loads with respect to motion also have a good agreement between experiment and theory.

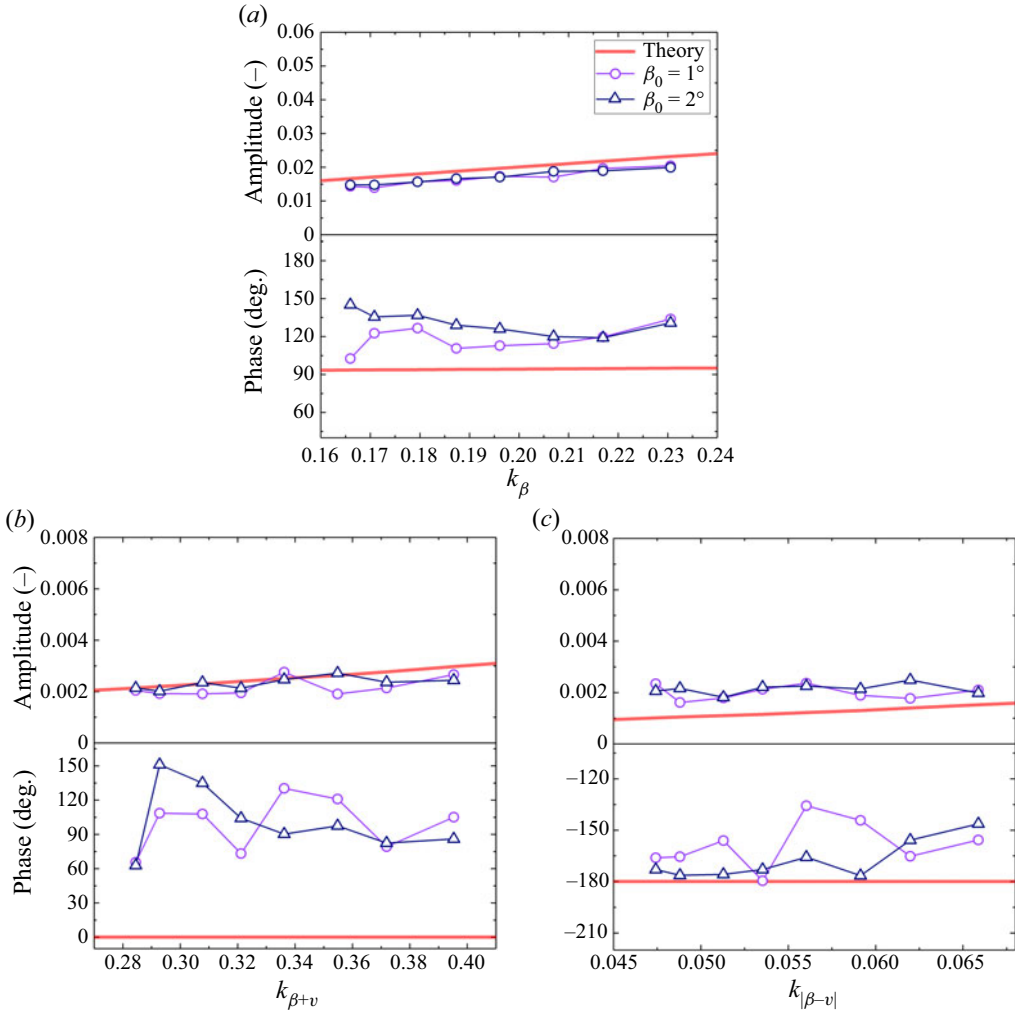

FIGURE 7. Normalized moment amplitudes of (*a*) pitch motion frequency f_β, (*b*) sum frequency f_{sum} and (*c*) difference frequency f_{diff} with different reduced frequency. Here $f_\beta = 1.4$ Hz, $k_\beta = 2\pi f_\beta b/v_0$, $k_{\beta+v} = 2\pi f_{sum} b/v_0$, $k_{|\beta-v|} = 2\pi f_{diff} b/v_0$.

Figures 7(*b*) and 8(*b*) present the results of the sum frequency component. The amplitudes obtained by the experiment still agree well with Greenberg's prediction while a significant difference is observed for the phase plots. For the difference frequency component shown in figures 7(*c*) and 8(*c*), the differences of amplitudes between the experimental results and theoretical prediction are relatively marked. However, the experimental results of phase angles agree well with the theoretical values. It can be concluded that the amplitudes of moment coefficient of the experimental results agree reasonably well with the theoretical prediction, which is similar to that for lift coefficients.

Figure 9 shows the lift amplitudes and phase angles of flow frequency component with different reduced frequencies. To compare the magnitude between different β_0, the lift amplitudes are normalized by $2\pi\rho b v_0{}^2$, and thus the effect of pitching amplitude β_0 is considered. In each group of plots, it is clear that the amplitudes decrease slowly

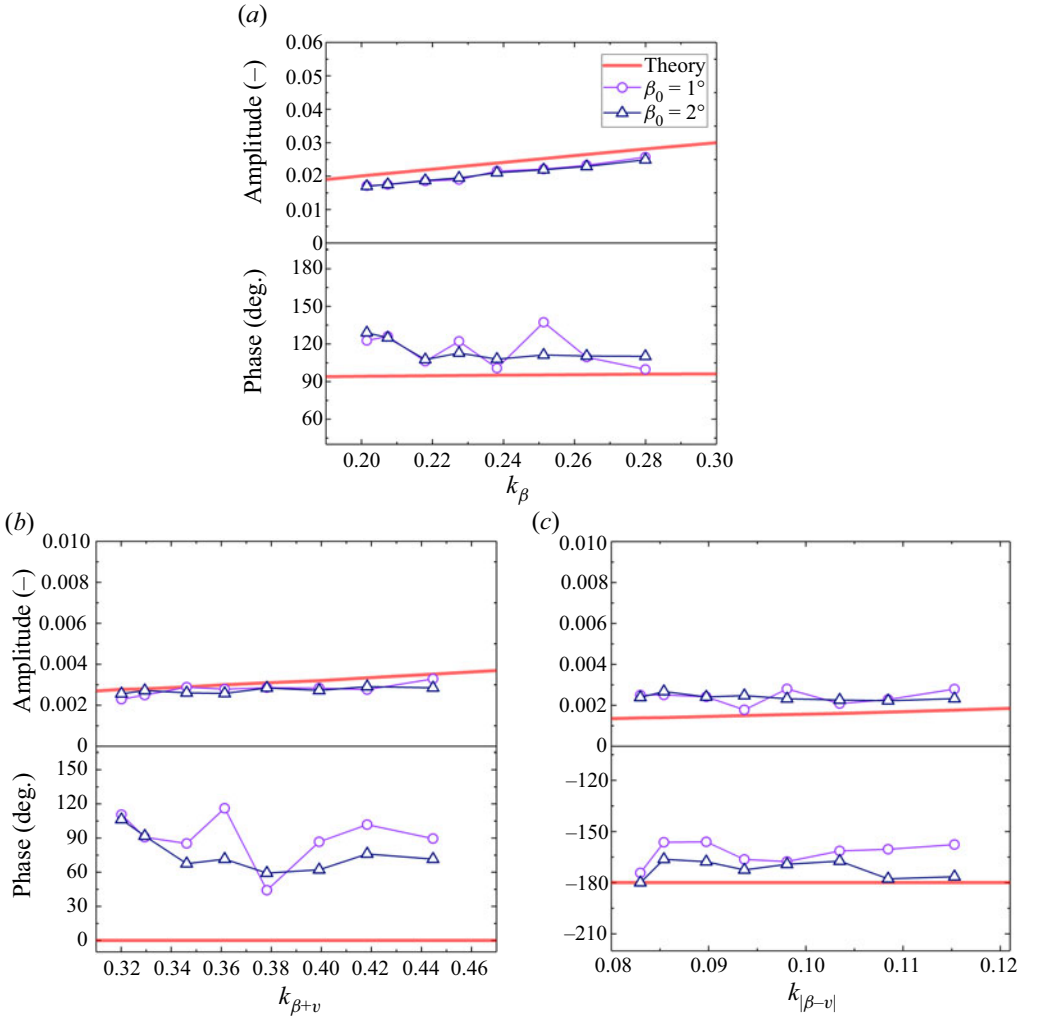

FIGURE 8. Normalized moment amplitudes of (*a*) pitch motion frequency f_β, (*b*) sum frequency f_{sum} and (*c*) difference frequency f_{diff} with different reduced frequency. Here $f_\beta = 1.7$ Hz, $k_\beta = 2\pi f_\beta b/v_0$, $k_{\beta+v} = 2\pi f_{sum} b/v_0$, $k_{|\beta-v|} = 2\pi f_{diff} b/v_0$.

with the increase of reduced frequency while the phase angles remain almost unchanged. The amplitudes for $\beta_0 = 1^\circ$ are nearly equal to those for 2°. This implies that the pitching amplitude β_0 has almost no effect on this frequency component. Moreover, the amplitudes for $f_\beta = 1.4$ Hz in figure 9(*a*) are identical to those for $f_\beta = 1.7$ Hz in figure 9(*b*), which implies that the pitch frequency f_β also has no effect on this frequency component. It seems that the flow frequency component is only affected by the incoming flow. As we discussed before, the reason causing this frequency component is probably due to the existence of a small steady attack angle, which is almost inevitable in such an actively controlled wind tunnel. Greenberg (1947) discussed the lift force caused by a steady attack angle. According to his theory, this component should not be affected by the forms of motion but by the incoming flow and the steady attack angle. This is in accordance with

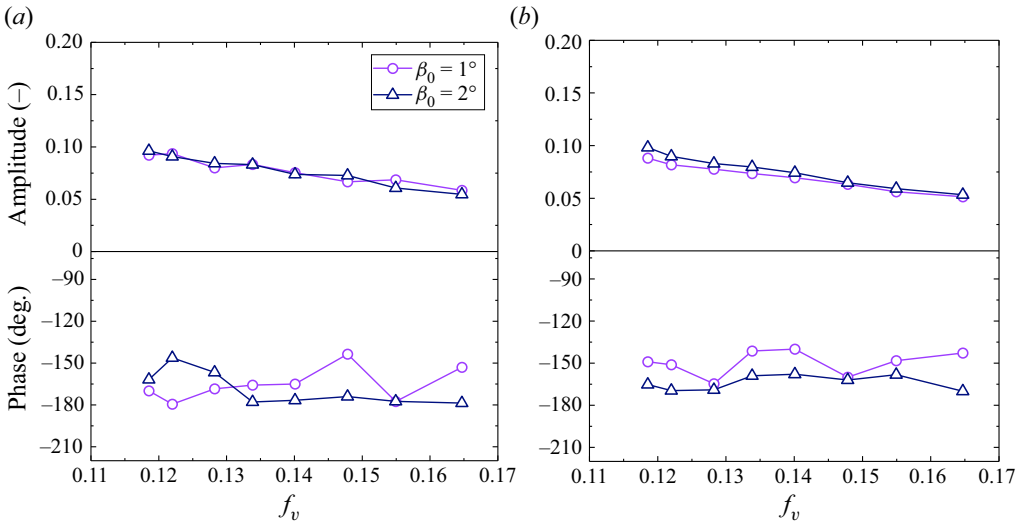

FIGURE 9. Normalized lift amplitudes and phase angles of gust frequency with different reduced frequencies: (*a*) $f_\beta = 1.4$ Hz; (*b*) $f_\beta = 1.7$ Hz. Here $f_v = 1$ Hz, $k_v = 2\pi f_v b/v_0$.

the experimental results. The validity of Greenberg's theory for a steady attack angle has been discussed by van der Wall & Leishman (1994) and Strangfeld *et al.* (2016).

5. Conclusion

A sinusoidal streamwise gust of high quality was generated by the multiple-fan actively controlled wind tunnel. Using the forced-oscillation rig, a NACA0015 airfoil oscillated in the wind tunnel test. In the case of an oscillating airfoil ($f_\beta = 1.4$ and 1.7 Hz, $\beta_0 = 1°$ and $2°$) encountering the sinusoidal streamwise gust with different oscillating frequencies ($f_v = 1$Hz, $\sigma = 0.2$), the unsteady lift force was measured by DMS-4000 pressure scanners, and compared with Greenberg's theoretical prediction. It was found that the experimental results agree generally well with the theoretical values. Through spectral analysis, it can be concluded that there are two main reasons for the small deviation between the experimental and theoretical values. First, the component of gust frequency caused by the small steady attack angle, which is almost inevitable in such an actively controlled wind tunnel, is likely to have a small effect. This could be the reason for the poorer agreement for the component of difference frequency. Second, the thickness of the NACA0015 airfoil may have a small effect on the lift and moment, which has been discussed by many researchers.

In conclusion, the sum frequency $f_{sum} = f_\beta + f_v$ and the difference frequency $f_{diff} = |f_\beta - f_v|$ discussed by Greenberg (1947) are confirmed to exist as determined through spectral analysis. This is probably the first time for these two frequencies being observed in experiments. It can be concluded that the agreement between theory and experiment is best for the frequency component of pitching frequency, and still reasonably good for the sum frequency component and least good for the difference frequency component, since that is also the order of the relative magnitudes of the lifts at each of these frequency components. In general, the experimental results for unsteady lift force of the oscillating airfoil in the sinusoidal streamwise gust with a small amplitude ($\sigma = 0.2$) agree well with Greenberg's

prediction, while there is a small difference. The main reasons for the deviation may be the thickness of the airfoil and the steady attack angle. In further works, experiments of an oscillating airfoil with an attack angle will be carried out to study the effect of the attack angle. For an oscillating airfoil encountering a sinusoidal streamwise gust of arbitrary oscillating frequency, Greenberg's theory appears to be an appropriate approach.

Acknowledgements

This work was funded by the National Natural Science Foundation of China under grant no. 51878580.

Declaration of interests

The authors report no conflict of interest.

REFERENCES

BARLAS, T. K. & VAN KUIK, G. A. M. 2010 Review of state of the art in smart rotor control research for wind turbines. *Prog. Aerosp. Sci.* **46** (1), 1–27.

FAVIER, D., AGNES, A., BARBI, C. & MARESCA, C. 1988 Combined translation/pitch motion – a new airfoil dynamic stall simulation. *J. Aircraft* **25** (9), 805–814.

GLEGG, S. A. L. & DEVENPORT, W. 2009 Unsteady loading on an airfoil of arbitrary thickness. *J. Sound Vib.* **319** (3–5), 1252–1270.

GRANLUND, K., MONNIER, B., OL, M. & WILLIAMS, D. 2014 Airfoil longitudinal gust response in separated vs. attached flows. *Phys. Fluids* **26** (2), 1–14.

GREENBERG, J. M. 1947 Airfoil in sinusoidal motion in a pulsating stream. *NACA Tech. Rep.* TN1326. National Advisory Committee for Aeronautics.

HALFMAN, R. L. 1952 Experimental aerodynamic derivatives of a sinusoidally oscillating airfoil in two-dimensional flow. *NACA Tech. Rep.* 1108. National Advisory Committee for Aeronautics.

HARDING, S. F., PAYNE, G. S. & BRYDEN, I. G. 2014 Generating controllable velocity fluctuations using twin oscillating hydrofoils: experimental validation. *J. Fluid Mech.* **750**, 113–123.

ISAACS, R. 1945 Airfoil theory for flows of variable velocity. *J. Aeronaut. Sci.* **12** (1), 113–117.

JOHNSON, W. 1980 Application of unsteady airfoil theory to rotary wings. *J. Aircraft* **17** (4), 285–286.

VON KARMAN, T. & SEARS, W. R. 1938 Airfoil theory for nonuniform motion. *J. Aeronaut. Sci.* **5**, 379–390.

KEMP, N. H. & SEARS, W. R. 1953 Aerodynamic interference between moving blade rows. *J. Aeronaut. Sci.* **20**, 585–598.

KEMP, N. H. & SEARS, W. R. 1955 The unsteady forces due to viscous wakes in turbomachines. *J. Aeronaut. Sci.* **22**, 478–483.

KERSTENS, W., PFEIFFER, J., WILLIAMS, D., KING, R. & COLONIUS, T. 2011 Closed-loop control of lift for longitudinal gust suppression at low Reynolds numbers. *AIAA J.* **49** (8), 1721–1728.

KOTTAPALLI, S. B. R. 1985 Technical notes: unsteady aerodynamics of oscillating airfoils with inplane motions. *J. Am. Helicopter Soc.* **30** (1), 62–63.

VAN KUIK, G. A. M., MICALLEF, D., HERRAEZ, I., VAN ZUIJLEN, A. H. & RAGNI, D. 2014 The role of conservative forces in rotor aerodynamics. *J. Fluid Mech.* **750** (5), 284–315.

LEISHMAN, J. G. 2002 Challenges in modelling the unsteady aerodynamics of wind turbines. *Wind Energy* **5** (2–3), 85–132.

MONNIER, B., WILLIAMS, D. R., WEIER, T. & ALBRECHT, T. 2016 Comparison of a separated flow response to localized and global-type disturbances. *Exp. Fluids* **57** (7), 114.

MOTTA, V., GUARDONE, A. & QUARANTA, G. 2015 Influence of airfoil thickness on unsteady aerodynamic loads on pitching airfoils. *J. Fluid Mech.* **774**, 460–487.

RAINEY, A. G. 1957 Measurement of aerodynamic forces for various mean angles of attack on an airfoil oscillating in pitch and on two finite-span wings oscillating in bending with emphasis on damping in the stall. *NACA Tech. Rep.* 1305. National Advisory Committee for Aeronautics.

REID, E. G. 1940 An experimental determination of the lift of an oscillating airfoil. *J. Aero. Sci.* **8** (1), 1–6.

SEARS, W. R. 1941 Some aspects of non-stationary airfoil theory and its practical application. *J. Aeronaut. Sci.* **8** (3), 104–108.

SILVERSTEIN, A. & JOYNER, U. T. 1939 Experimental verification of the theory of oscillating airfoils. *NACA Tech. Rep.* 673. National Advisory Committee for Aeronautics.

STRANGFELD, C., MÜLLER-VAHL, H., NAYERI, C. N., PASCHEREIT, C. O. & GREENBLATT, D. 2016 Airfoil in a high amplitude oscillating stream. *J. Fluid Mech.* **793**, 79–108.

STRANGFELD, C., RUMSEY, C. L., MUELLER-VAHL, H., GREENBLATT, D., NAYERI, C. N. & PASCHEREIT, C. O. 2015 Unsteady thick airfoil aerodynamics: experiments, computation, and theory. In *AIAA Paper 2015-3071, 45th AIAA Fluid Dynamics Conference*. American Institute of Aeronautics and Astronautics.

SZUMOWSKI, A. P. & MEIER, G. E. A. 1996 Forced oscillations of airfoil flows. *Exp. Fluids* **21** (6), 457–464.

THEODORSEN, T. 1935 General theory of aerodynamic instability and the mechanism of flutter. *NACA Tech. Rep.* 496, pp. 413–433. National Advisory Committee for Aeronautics.

VAN DER WALL, B. G. & LEISHMAN, J. G. 1994 On the influence of time-varying flow velocity on unsteady aerodynamics. *J. Am. Helicopter Soc.* **39** (4), 25.

YANG, Y., LI, M., MA, C. & LI, S. 2017 Experimental investigation on the unsteady lift of an airfoil in a sinusoidal streamwise gust. *Phys. Fluids* **29** (5), 051703.